Identification and Description of Copper-Thiolate Vibrations in the Dinuclear Cu_A Site of Cytochrome *c* Oxidase

Colin R. Andrew,[1a] Robert Fraczkiewicz,[1b] Roman S. Czernuszewicz,[1b] Pekka Lappalainen,[1c] Matti Saraste,[1c] and Joann Sanders-Loehr*,[1a]

Contribution from the Department of Chemistry, Biochemistry, and Molecular Biology, Oregon Graduate Institute of Science & Technology, Portland, Oregon 97291-1000, Department of Chemistry, University of Houston, Houston, Texas 77204, and European Molecular Biology Laboratory, Meyerhofstrasse 1, Postfach 10.2209, D-69012 Heidelberg, Germany.

Received March 25, 1996[⊗]

Abstract: The Cu_A site of cytochrome *c* oxidase and the type 1 Cu site of cupredoxins occur in homologous protein folds with a His_2Cys ligand set, but are distinguished by the presence of a second Cys and a second Cu in Cu_A that result in the formation of a dithiolate-bridged dinuclear Cu cluster. The resonance Raman (RR) spectrum of the soluble Cu_A-containing fragment from *Paracoccus denitrificans* exhibits intense vibrations at 260 and 339 cm^{-1}. Their respective ^{34}S-isotope shifts of −4.1 and −5.1 cm^{-1} allow them to be assigned to two Cu−S stretching modes, ν(Cu−S), of the $Cu_2S_2Im_2$ moiety. A normal coordinate analysis (NCA) of the RR spectra of Cu_A substituted with isotopes of S, Cu, and N was carried out to determine whether it is possible to distinguish between dinuclear models with bridging or terminal cysteine ligands. Whereas the terminal Cys model predicts that both of the ν(Cu−S) modes lie between 340 and 350 cm^{-1}, the bridging Cys geometry successfully predicts the S-shifts at 260 and 339 cm^{-1}. Thus, the Raman data and NCA are fully consistent with the bridging cysteine coordination observed by X-ray crystallography. The agreement between predicted and observed vibrational isotope data is further improved by a *trans*-tilting of the imidazole nitrogens above and below the Cu_2S_2 plane, yielding a distorted tetrahedral geometry for each of the Cu atoms. Whereas type 1 protein RR spectra are highly N-dependent due to extended vibronic coupling with amide vibrations of the cysteine ligand, the vibrations in Cu_A are relatively insensitive to N-isotope substitution. Thus, unlike type 1 Cu, the RR spectrum of Cu_A can be successfully modeled with only the $Cu_2S_2(Im)_2$ core.

Introduction

Cytochrome *c* oxidase (CCO) catalyses the reduction of dioxygen to water in the final step of the respiratory chain in mitochondria and many aerobic bacteria.[2] The Cu_A center accepts reducing equivalents from cytochrome *c* and passes them via intramolecular electron transfer to a low-spin heme Fe_a and finally to a dinuclear heme Fe_{a3}/Cu_B site where the reduction of O_2 to H_2O takes place. Because of its location within the membrane-bound cytochrome *c* oxidase, the Cu_A site has resisted spectroscopic and structural characterization owing to the strong spectral interference from the heme groups and the inherent difficulties of studying a membrane-bound enzyme. However, the genetic engineering of soluble Cu_A-containing CCO fragments from *Paracoccus denitrificans*,[3] *Bacillus subtilis*,[4] and *Thermus thermophilus*[5] bacteria has opened the door to unimpeded spectroscopic investigation and Cu-site manipulation through site-directed mutagenesis. In the same vein, recombinant DNA technology has been used to construct purple Cu_A centers in the CyoA subunit of a quinol oxidase from *Escherichia coli* (purple CyoA)[6,7] and in place of the type 1 Cu sites of *Pseudomonas aeruginosa* azurin[8] and *Thiobacillus versutus* amicyanin.[9] These constructs are apparently facilitated by all three proteins being evolutionarily related to the Cu_A domain of CCO.[6] Both the type 1 copper proteins and the Cu_A domains exhibit similar cupredoxin folds consisting of 10 stranded β-barrels, with several additional β strands being present in the Cu_A domains.[10]

Until recently, the question whether Cu_A was a mono- or dinuclear Cu center was hotly debated, and this controversy was fueled by uncertainties in elemental analysis. The major evidence for a dinuclear structure came from EPR spectroscopy, which led to the realization that Cu_A is a dinuclear mixed-valence system, similar to that of the A-site of nitrous oxide reductase (N_2OR).[11] Similar to N_2OR, all of the engineered Cu_A proteins[3−9] exhibit a seven-line EPR hyperfine pattern consistent with the delocalization of one unpaired electron over two copper ions to give an average valence of 1.5. Further indications of a dinuclear structure came from EXAFS studies of *B. subtilis* Cu_A which showed strong Cu−Cu scattering at 2.47 Å,[12] and they were corroborated by the EXAFS finding of a 2.46-Å distance for Cu_A in native mitochondrial CCO.[13]

⊗ Abstract published in *Advance ACS Abstracts,* October 15, 1996.

(1) (a) Oregon Graduate Institute. (b) University of Houston. (c) European Molecular Biology Laboratory.

(2) Babcock, G. T.; Wikström, M. *Nature* **1992**, *356*, 301−309.
(3) Lappalainen, P.; Aasa, R.; Malmström, B. G.; Saraste, M. *J. Biol. Chem.* **1993**, *268*, 26416−26421.
(4) von Wachenfeld, C.; de Vries, S.; van der Oost, J. *FEBS Lett.* **1994**, *340*, 109−113.
(5) Fee, J. A.; Sanders, D.; Slutter, C. E.; Doan, P. E.; Aasa, R.; Karpefors, M.; Vänngård, T. *Biochem. Biophys. Res. Commun.* **1995**, *212*, 77−83.
(6) van der Oost, J.; Lappalainen, P.; Musacchio, A.; Warne, A.; Lemieux, L.; Rumbley, J.; Gennis, R. B.; Aasa, R.; Pascher, T.; Malmström, B. G.; Saraste, M. *EMBO J.* **1992**, *11*, 3209−3217.
(7) Kelly, M.; Lappalainen, P.; Talbo, G.; Haltia, T.; van der Oost, J.; Saraste, M. *J. Biol. Chem.* **1993**, *268*, 16781−16787.
(8) Hay, M.; Richards, J. H.; Lu, Y. *Proc. Natl. Acad. Sci. U.S.A.* **1996**, *93*, 461−464.
(9) Dennison, C.; Vijgenboom, E.; de vries, S.; van der Oost, J.; Canters, G. W. *FEBS Lett.* **1995**, *365*, 92−94.
(10) Adman, E. T. *Nature Struct. Biol.* **1995**, *2*, 929−931.
(11) Antholine, W. E.; Kastrau, D. H. W.; Steffens, G. C. M.; Buse, G.; Zumft, W. G.; Kroneck, P. M. H. *Eur. J. Biochem.* **1992**, *209*, 875−881.
(12) Blackburn, N. J.; Barr, M. E.; Woodruff, W. H.; van der Oost, J.; de Vries, S. *Biochemistry* **1994**, *33*, 10401−10407.
(13) Henkel, G.; Müller, A.; Weissgräber, S.; Buse, G.; Soulimane, T.; Steffens, G. C. M.; Nolting, H.-F. *Angew. Chem. Int. Ed. Engl.* **1995**, *34*, 1488−1492.

S0002-7863(96)00969-9 CCC: $12.00

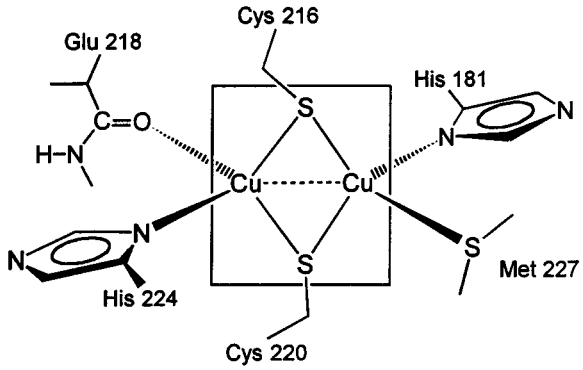

Figure 1. Idealized structure of the Cu_A site in the soluble fragment of *P. denitrificans* CCO, based on the X-ray structure of *P. denitrificans* CCO.[16] The S of Met 227 and backbone C═O of Glu 218 are only weakly coordinated. The dashed line indicates a possible Cu···Cu bond.

Based on the knowledge that the dinuclear site contains only four essential amino acid ligands (two Cys and two His), several symmetrical models were proposed: one with the copper ions linked by two bridging cysteine thiolates and one with terminal thiolates and a Cu−Cu bond.[14]

This dispute has been relatively well settled by the X-ray crystal structures of the Cu_A sites in purple CyoA,[15] *P. denitrificans* CCO,[16] and beef-heart mitochondrial CCO.[17] As shown in Figure 1, each Cu is coordinated by two bridging cysteinate sulfur atoms at a distance of ∼2.25 Å and one imidazole nitrogen at ∼1.95 Å, and the unusually short Cu−Cu distance of ∼2.55 Å is in agreement with that detected by EXAFS.[12] There are also weak axial interactions with a methionine sulfur and a peptide carbonyl oxygen from a glutamate residue on opposite sides of the Cu_2S_2 plane that cause a tetrahedral distortion of each of the copper centers. The unusually short Cu−Cu distance and small Cu−S−Cu angle of <70° raises the possibility of an additional Cu−Cu bonding interaction between the two coppers. There is also considerable interest in understanding the spectroscopic properties associated with this novel bridging-cysteinate coordination and how they differ from those of the mononuclear copper-cysteinate proteins.

Resonance Raman (RR) spectroscopy, a technique that selectively probes vibrations of the Cu−S(Cys) chromophore, provides an ideal method for characterizing copper-cysteinate sites.[18,19] For the *mononuclear* copper-cysteinate proteins, excitation within a (Cys)S→Cu CT band leads to the enhancement of five or more vibrational fundamentals between 250 and 500 cm^{-1}. These are believed to originate from vibronic and kinematic coupling of the Cu−S stretch with internal ligand deformations of the cysteine backbone.[20,21] Studies of an extensive series of copper-cysteinate proteins have shown that a *single, predominant* Cu−S stretching mode can be identified by its large frequency shift upon S- (or Cu-) isotope substitution, its high intensity, and its role as the generator of combination bands.[22,23] The frequency of the Cu−S(Cys) stretching vibration, ν(Cu−S), acts as a sensitive indicator of both the Cu−S bond length and the Cu-coordination geometry to a degree of accuracy that is well beyond the limits of X-ray crystallography. The variation in ν(Cu−S) frequencies has been used to define a continuum of coordination geometries among mononuclear copper-cysteinate proteins, ranging from trigonal planar (430−405 cm^{-1}) to tetrahedral (360−340 cm^{-1}) and tetragonal (320−300 cm^{-1}).[22]

The *dinuclear* copper-cysteinate sites (Cu_A in CCO, A in N_2-OR) give a significantly different pattern of RR modes with *two intense* Cu−S stretching modes near 260 and 340 cm^{-1}.[24,25] Both of these features are identified as ν(Cu−S) modes by their frequency shifts of −4 to −5 cm^{-1} with ^{34}S-substituted protein.[25] This is in contrast to the mononuclear copper-cysteinate proteins where the *single* predominant ν(Cu−S) mode exhibits a maximal ^{34}S-shift of only −2 to −4 cm^{-1}.[23,26] The greater isotope dependence of the two Cu−S stretching modes in the dinuclear Cu proteins suggests that they are due to relatively pure vibrations of the $Cu_2S_2(Im)_2$ moiety and have considerably less coupling with cysteine backbone deformations. In addition, the frequencies of these two vibrations are remarkably constant among all of the proteins that have been thus far examined: bovine heart mitochondrial CCO,[27,28] the Cu_A fragments from *B. subtilis*,[24] *P. denitrificans*, and *T. thermophilus*,[25] as well as the Cu_A constructs in *Ps. aeruginosa* azurin, *T. versutus* amicyanin,[25] and purple CyoA.[29] This indicates that the $Cu_2S_2(Im)_2$ structure is highly conserved among the different Cu_A sites.

To provide a firmer basis for these RR spectral assignments, we have now obtained data on the *P. denitrificans* Cu_A fragment substituted with isotopes of Cu, S, and N. The Cu- and N-isotope dependencies corroborate our conclusion that the vibrational motions in Cu_A are predominantly due to the Cu and S atoms, with much less coupling to the vibrations of the cysteinate side chain and polypeptide backbone than in the mononuclear copper-cysteinate proteins. This has made it possible to perform normal coordinate analysis (NCA) calculations and accurately fit the RR spectra to the vibrations of a $Cu_2S_2(Im)_2$ core. This NCA supports the crystallographic evidence for a bridging thiolate structure and a tetrahedral Cu coordination geometry in Cu_A.

Experimental Procedures

Protein Samples. The Cu_A-containing domain of *P. denitrificans* cytochrome *c* oxidase was expressed in *E. coli* as described previously.[3] To fully label the protein with ^{34}S, cells were grown on minimal medium

(14) Farrar, J. A.; Lappalainen, P.; Zumft, W. G.; Saraste, M.; Thomson, A. J. *Eur. J. Biochem.* **1995**, *232*, 294−303.
(15) Wilmanns, M.; Lappalainen, P.; Kelly, M.; Sauer-Eriksson, E.; Saraste, M. *Proc. Natl. Acad. Sci. U.S.A.* **1995**, *92*, 11955−11959.
(16) Iwata, S.; Ostermeier, C.; Ludwig, B.; Michel, H. *Nature* **1995**, *376*, 660−669.
(17) Tsukihara, T.; Aoyama, H.; Yamashita, E.; Tomizaki, T.; Yamaguchi, H.; Shinzawa-Itoh, K.; Nakashima, R.; Yaono, R.; Yoshikawa, S. *Science* **1995**, *269*, 1069−1074.
(18) Woodruff, W. H.; Dyer, R. B.; Schoonover, J. R. In *Biological Applications of Raman Spectroscopy*; Spiro, T. G., Ed.; Wiley: New York, 1988; Vol. 3, pp 413−438.
(19) Andrew, C. R.; Sanders-Loehr, J. *Acc. Chem. Res.* **1996**, *29*, 365−372.
(20) Nestor, L.; Larrabee, J. A.; Woolery, G.; Reinhammar, B.; Spiro, T. G. *Biochemistry* **1984**, *23*, 1084−1093.
(21) Han, J.; Adman, E. T.; Beppu, T.; Codd, R.; Freeman, H. C.; Huq, L.; Loehr, T. M.; Sanders-Loehr, J. *Biochemistry* **1991**, *30*, 10904−10913.
(22) Andrew, C. R.; Yeom, H.; Valentine, J. S.; Karlsson, B. G.; Bonander, N.; van Pouderoyen, G.; Canters, G. W.; Loehr, T. M.; Sanders-Loehr, J. *J. Am. Chem. Soc.* **1994**, *116*, 11489−11498.
(23) Dave, B. C.; Germanas, J. P.; Czernuszewicz, R. S. *J. Am. Chem. Soc.* **1993**, *115*, 12175−12176.
(24) Andrew, C. R.; Han, J.; de Vries, S.; van der Oost, J.; Averill, B. A.; Loehr, T. M.; Sanders-Loehr, J. *J. Am. Chem. Soc.* **1994**, *116*, 10805−10806.
(25) Andrew, C. R.; Lappalainen, P.; Saraste, M.; Hay, M. T.; Lu, Y.; Dennison, C.; Canters, G. W.; Fee, J. A.; Slutter, C. E.; Nakamura, N.; Sanders-Loehr, J. *J. Am. Chem. Soc.* **1995**, *117*, 10759−10760.
(26) Qiu, D.; Dong, S.; Ybe, J. A.; Hecht, M. H.; Spiro, T. G. *J. Am. Chem. Soc.* **1995**, *117*, 6443−6446.
(27) Takahashi, S.; Ogura, T.; Shinzawa-Itoh, K.; Yoshikawa, S.; Kitagawa, T. *Biochemistry* **1993**, *32*, 3664−3670.
(28) Wallace-Williams, S. E.; James, C. A.; de Vries, S.; Saraste, M.; Lappalainen, P.; van der Oost, J.; Fabian, M.; Palmer, G.; Woodruff, W. H. *J. Am. Chem. Soc.* **1996**, *118*, 3986−3987.
(29) Andrew, C. R.; Nakamura, N.; Sanders-Loehr, J.; Saraste, M. Unpublished results.

containing 1 mL/L of a trace element solution[30] and 1 mM $Na_2{}^{34}SO_4$ (90 atom %, ICON). Substitution of all protein nitrogen with ^{15}N was achieved by growing cells on M9 minimal medium[31] containing 10 mM $^{15}NH_4Cl$. Incorporation of copper isotopes was accomplished on freshly isolated apoprotein (15 μM) by first reducing the cysteine residues with a 3-h dialysis against 20 mM Tris, 1 mM DTT (pH 8.2), followed by a 1-h dialysis against 20 mM Tris (pH 8.2). The sample was then dialyzed for 3 h against 5 vol of 20 mM Tris (pH 8.2) containing 50 μM $^{63}Cu(NO_3)_2$ or $^{65}Cu(NO_3)_2$, followed by a 3-h dialysis against 20 mM Bis-Tris (pH 6.5). The Cu solutions were prepared by dissolving 10 mg of metallic copper (99.7% ^{63}Cu or 99.2% ^{65}Cu, Intersales-Holland, BV) in 50 μL of 70% HNO_3, followed by 100-fold dilution and adjustment to pH 2 (for storage) and a 500-fold dilution in buffer.

The pH 10 form and the His224Asn mutant of the *P. denitrificans* Cu_A fragment were prepared as described previously.[3,14] The His224Asn mutant was originally ascribed to His 252 using numbering based on the cDNA sequence, but it corresponds to His 224 in the post-translationally processed protein (Figure 1).

Raman Spectroscopy. Raman spectra were obtained with a custom McPherson 2061/207 spectrograph (0.67 m, 1800-groove grating) and a Princeton Instruments (LN-1100PB) liquid N_2-cooled CCD detector. Rayleigh scattering was attenuated using either a Kaiser Optical holographic super-notch filter or a McPherson 270 double monochromator (600-groove grating) pre-filter stage. Excitation was provided by a Coherent Innova 90-6 Ar laser. Raman spectra were collected in an ~150° backscattering geometry from samples maintained at 15 K by use of a closed-cycle helium refrigerator (Air Products, Displex).[32] Absolute frequencies, obtained by calibration with CCl_4 or indene, are accurate to ± 1 cm^{-1}. Isotope shifts, obtained from spectra recorded under identical experimental conditions, have been evaluated by abscissa expansion and curve resolution of overlapping bands and are accurate to ± 0.5 cm^{-1}.

Normal Coordinate Analysis. Normal mode calculations were performed by the Wilson's **GF**-matrix method using a general valence force field.[33] All calculations were carried out on a Silicon Graphics INDY workstation using a UNIX version of a new NCA software package[34] to construct the **G** and **F** matrices and to solve the secular equations.[33] Force constants were refined by a newly developed procedure for refinement of harmonic vibrational force fields, free of regularization error and divergence problems.[34,35] Initial values of force constants were estimated from previously calculated force fields for coordinated copper.[36] In-plane bending, out-of-plane wag, and torsion principal force constants were also included to maintain the full rank of the **F**-matrix. The visualization of normal eigenvectors was accomplished by transfer of the Cartesian atomic displacements into the X-Mol molecular graphics program.[37]

Results and Discussion

The purple color of the Cu_A site arises from two intense absorption bands at 480 and 530 nm (ϵ = 3.0 and 2.6 mM^{-1} cm^{-1}), together with an unusually intense far-red absorption near 800 nm (ϵ = 1.6 mM^{-1} cm^{-1}).[3] All three absorption bands have substantial (Cys)S→Cu charge-transfer character, as demonstrated by the fact that excitation within any one of them produces a similar Raman spectrum with resonance enhancement of the Cu−S(Cys) stretching modes.[24] For example, excitation into either the 480- or 530-nm absorption band of *P. denitrificans* Cu_A results in the same set of RR frequencies with only minor changes in peak intensities (Figure 2).

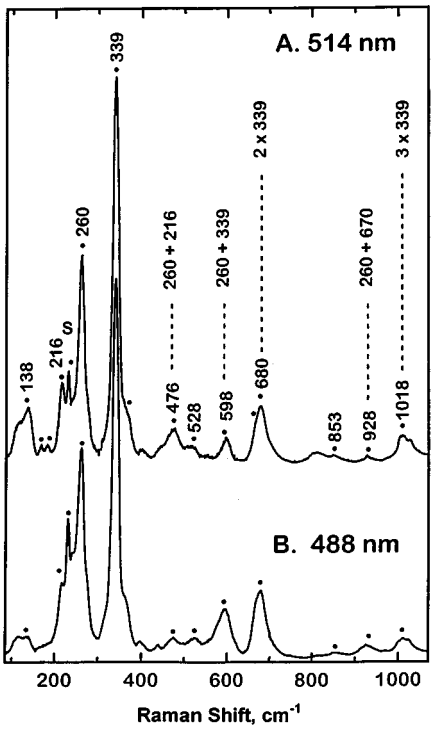

Figure 2. Resonance Raman spectra of the soluble Cu_A fragment of *P. denitrificans* CCO obtained with (A) 514-nm and (B) 488-nm excitation. Spectra were recorded on 2 mM protein in 20 mM Bis-Tris (pH 6.5) at 15 K using ~100 mW power, 1800-groove grating, 3-cm^{-1} slit width, and 20 min accumulation. *S* = frozen solvent. Overtones and combination bands are identified (- - -) by the sum of their constituent fundamentals.

For the mononuclear copper-cysteinate proteins with distorted tetrahedral type 1 sites, Cu−S stretching character is marked by S-isotope sensitivity, high intensity, and the ability to generate combination and overtone bands.[22] These same three properties are evident in the RR spectra of Cu_A sites. Thus, the RR spectrum of *P. denitrificans* Cu_A is dominated by ν(Cu−S) fundamentals at 260 and 339 cm^{-1} (Figure 2), which are S-isotope dependent and constitute the hallmark of Cu_A.[25] At least five other weaker fundamental modes occur between 100 and 400 cm^{-1}. The large number of additional features in the region above 400 cm^{-1} are due mainly to overtone and combination bands generated by the ν(Cu−S) modes, with overtones arising from the 339-cm^{-1} fundamental and combinations arising from the 260-cm^{-1} fundamental (Figure 2). Furthermore, an almost identical set of RR frequencies is observed for the Cu_A fragments from *B. subtilis* and *T. thermophilus* (Table 1). The validity of the vibrational assignments for all three proteins is supported by the isotope shifts discussed below.

Sulfur-Isotope Dependence. Isotopic substitution of the cysteine sulfur atom provides the most definitive means for identifying Cu−S(Cys) stretching vibrations. In the present study, the Cu_A protein was uniformly labeled by growing *P. denitrificans* on a minimal medium with $Na_2{}^{32}SO_4$ or $Na_2{}^{34}SO_4$ as the only sulfur source. Although this technique labels the Met227 ligand as well as the two Cys ligands, the methionine sulfur is not expected to be RR active based on its weak Cu interaction (bond length of 2.7 Å)[16] and the failure to observe any RR vibrations from the analogous Cu−S(Met) moiety in

(30) Jeter, R. M.; Ingraham, J. L. *Arch. Microbiol.* **1984**, *138*, 124−130.
(31) Sambrook, J.; Fritsch, E. F.; Maniatis, T. *Molecular Cloning: A Laboratory Manual*; Cold Spring Harbor Laboratory Press: Cold Spring Harbor, NY, 1989.
(32) Loehr, T. M.; Sanders-Loehr, J. *Methods Enzymol.* **1993**, *226*, 431−470.
(33) Wilson, E. B.; Decius, J. C.; Cross, P. C. *Molecular Vibrations: The Theory of Infrared and Raman Spectra*; Dover: New York, 1955.
(34) Fraczkiewicz, R. Ph.D. Thesis, University of Houston, 1996.
(35) Fraczkiewicz, R.; Czernuszewicz, R. S. Manuscript in preparation.
(36) Nakamoto, K. *Infrared and Raman Spectra of Inorganic and Coordination Compounds*; John Wiley and Sons: New York, 1986.
(37) *X-Mol, version 1.3.1*; Minnesota Supercomputer Center, Inc.: Minneapolis, MN, 1993.

Table 1. Observed Raman Frequencies and Isotope Shifts for Cu_A Fragments[a]

P. denitrificans				*B. subtilis*		*T. thermophilus*		assignment[b]		
freq	$\Delta^{34}S$	$\Delta^{65}Cu$	$\Delta^{15}N$	freq	$\Delta^{65}Cu$	freq	$\Delta^{65}Cu$	freq[b]	sym[c]	description[c]
115						116		**a**	B_g	
138	0	−1.4	0	124	−2.3[d]	134	−2	**b**	A_g	ν(Cu−Cu)
216	−1.5	−0.8	−1.6	213		219	0	**c**	B_u	
260	−4.1	−0.6	−0.4	**258**	−1.0	**264**	−0.7	**d**	A_g	ν(Cu−N)
275				272		274		**e**	B_g	
339	−5.1	−1.0	0	**340**	−1.7	**338**	−1.4	**f**	A_g	ν(Cu−S)
365						366	0	**g**	A_u	
476	−5	−2	−1.5			481		**d + c**		
528				518		520	−1.1	**2d**		
598	−9	−2	−0.6	598		601	−2.4	**d + f**		
670						667	−0.7	**h**		
680	−10	−2	0	679		678		**2f**		
928	−7	−2	0					**d + h**		
1018	−16	−2	0	1019				**3f**		

[a] Frequencies in cm^{-1} with most intense peaks in boldface. Frequency shifts to lower energy (Δ) in presence of heavier isotope, as described in Figure 3. Data for *B. subtilis* and *T. thermophilus* Cu_A obtained with 488-nm excitation as previously published.[24,25] [b] Frequencies for overtones and combinations from isotope dependence. [c] Assignment based on NCA for the B_2 bridging model (Table 3) using C_{2h} symmetry, and the description is for the major PED contributor. [d] Data at 15 K using 825-nm excitation from ref 28.

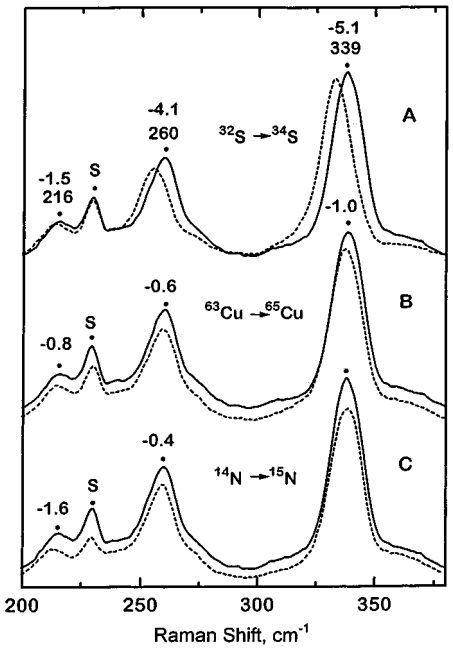

Figure 3. Effect of isotope substitution on RR spectrum of *P. denitrificans* Cu_A. (A) Cu_A fragment from cells grown on [^{32}S]- or [^{34}S]sulfate. (B) Cu_A apoprotein fragment reconstituted with ^{63}Cu or ^{65}Cu. (C) Cu_A fragment from cells grown on [^{14}N]- or [^{15}N]ammonium chloride. Spectra were recorded as in Figure 2 using 488-nm (∼40 mW) excitation and 10-min data accumulation. Peak frequencies are listed for the lighter isotope spectra (—) with frequency shifts for the heavier isotope spectra (- - -) indicated above.

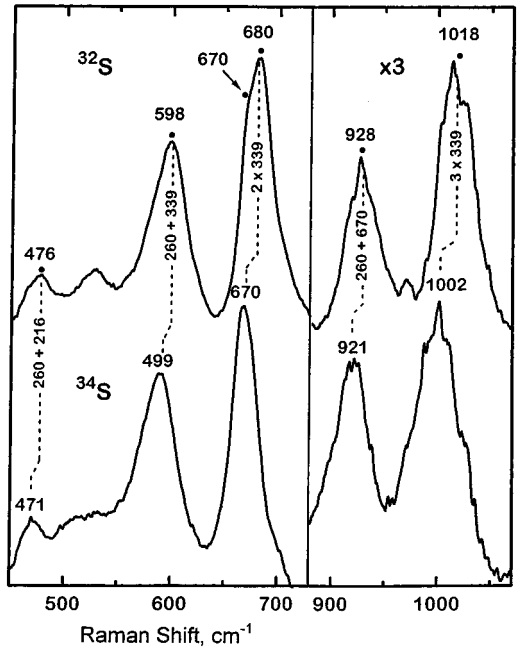

Figure 4. Combination and overtone bands in RR spectrum of *P. denitrificans* Cu_A from cells grown on [^{32}S]- or [^{34}S]sulfate. Spectra obtained as in Figure 2 using 488-nm excitation.

the type 1 site of azurin.[38] Thus, the large frequency shifts of −4.1 and −5.1 cm^{-1}, respectively, upon substitution of ^{34}S for ^{32}S (Figure 3A) identify the 260- and 339-cm^{-1} features as Cu−S(Cys) stretching modes. Further evidence for these assignments comes from the isotope dependence in the overtone region. The overtone progression of the 339-cm^{-1} fundamental with bands at 680 (2 × 339) and 1018 (3 × 339) cm^{-1} is confirmed by S-isotope shifts of −5, −10, and −16 cm^{-1}, respectively (Table 1, Figure 4). Similarly, the involvement of the 260-cm^{-1} fundamental in the generation of combination bands at 476 (260 + 216), 598 (260 + 339), and 928 (260 + 670) cm^{-1} is confirmed by S-isotope shifts of −5, −9, and −7 cm^{-1}, respectively (Table 1, Figure 4).

A comparison of S-isotope shifts in the RR spectra of Cu_A and type 1 Cu proteins highlights important distinctions arising from their different modes of cysteine coordination (Figure 5). In proteins such as azurin[23] and plastocyanin[26] with a single terminal cysteinate, multiple S-dependent bands are generated by kinematic coupling of a *single* Cu−S stretch with Cys ligand deformation modes of similar energy.[20,21] For example in azurin, total S-isotope shifts of ∼6 cm^{-1} are distributed within ∼30 cm^{-1} of the predominant ν(Cu−S) mode at 408 cm^{-1}, forming a cluster of bands with Cu−S stretching character (Figure 5B). In contrast, the bridging cysteinates in *P. denitrificans* Cu_A produce an increased total S-isotope shift of ∼11 cm^{-1} and a larger energy separation of ∼80 cm^{-1} between the 260- and 339-cm^{-1} modes (Figure 5A). The appearance of a single S-dependent mode at 339 cm^{-1} with a large shift of −5.1 cm^{-1} and no other S-dependent modes of similar energy indicates that it is a fairly pure Cu−S stretch with little kinematic coupling to Cys ligand deformation modes. Thus, the well-separated S-dependent modes of Cu_A are best ascribed to *multiple* Cu−S

(38) Thamann, T. J.; Willis, L. J.; Loehr, T. M. *Proc. Natl. Acad. Sci. U.S.A.* **1982**, *79*, 6396−6400.

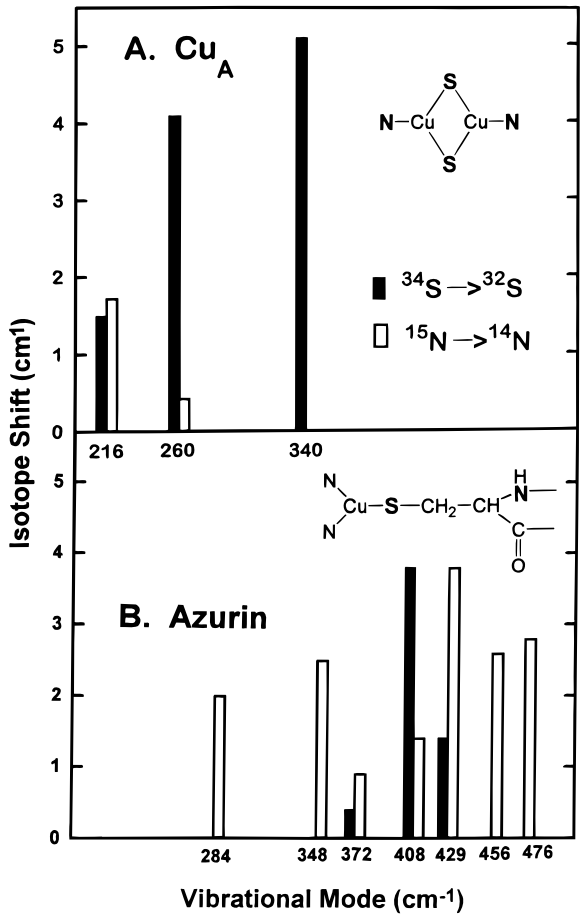

Figure 5. Sulfur- and nitrogen-isotope dependence of individual Raman modes. Proteins were obtained from cells grown on [^{32}S]- or [^{34}S]sulfate and [^{14}N]- or [^{15}N]ammonium chloride. (A) Cu_A fragment from *P. denitrificans* (data from Figure 3, panels A and C). (B) Azurin from *Ps. aeruginosa* (S-isotope data from ref 23, N-isotope data from ref 40). Atoms in boldface are those believed to be responsible for isotope shifts.

stretching modes originating from the presence of two bridging thiolate ligands.

Copper-Isotope Dependence. As Cu has a larger mass than S, frequency shifts upon substitution of ^{65}Cu for ^{63}Cu are smaller than for substitution of ^{34}S for ^{32}S. For type 1 Cu proteins such as azurin and plastocyanin, ^{65}Cu-shifts are observed for the same vibrational modes as S-isotope shifts (Figure 5) but typically with values of only -1 cm^{-1} or less[26,39] as compared to values of -2 to -4 cm^{-1} for the ^{34}S-shifts. Similarly in the case of the Cu_A-containing proteins, the ν(Cu−S) modes at 260 and 339 cm^{-1} undergo ^{65}Cu-shifts of -0.6 and -1.0 cm^{-1}, respectively, for *P. denitrificans* (Figure 3B), -1.0 and -1.7 cm^{-1} for *B. subtilis*, and -0.7 and -1.4 cm^{-1} for *T. thermophilus* (Table 1). As expected, these ^{65}Cu-shifts are considerably smaller than ^{34}S-shifts of -4.1 and -5.1 cm^{-1} for these same vibrational modes. In contrast, the 138-cm^{-1} fundamental of *P. denitrificans* Cu_A exhibits a quite large ^{65}Cu-shift of -1.4 cm^{-1}, with no corresponding S-isotope shift being detected (Table 1). Equally large ^{65}Cu-shifts have been observed for the 134-cm^{-1} mode of *T. thermophilus* Cu_A (Table 1) and the 124-cm^{-1} mode of *B. subtilis* Cu_A.[28] The unusual Cu-isotope dependence of this low-frequency mode as well as its preferential enhancement within the 800-nm absorption band led to the suggestion that the ∼130-cm^{-1} vibration has substantial Cu−Cu stretching character.[28]

Nitrogen-Isotope Dependence. The complete labeling of all nitrogens, including the imidazole rings of His and the polypeptide backbone, can been achieved by growing bacteria on $^{15}NH_4Cl$. For the type 1 Cu protein azurin from *Ps. aeruginosa*, ^{15}N substitution leads to shifts of -1 to -4 cm^{-1} in at least seven different fundamentals between 250 and 500 cm^{-1}(Figure 5B).[40] Similar ^{15}N-shifts have been observed for the type 1 Cu protein, plastocyanin, uniformly labeled by growth on $^{15}NH_4Cl$.[26] Selective labeling of the imidazole ring has been made possible through the availability of the azurin ligand mutants, His46Gly and His117Gly, which can be reconstituted with exogenous imidazole to generate type 1 Cu sites almost indistinguishable from the wild-type protein.[41,42] Reconstitution with [^{15}N]- versus [^{14}N]imidazole causes no detectable frequency shifts in the RR spectrum of either the His46Gly or the His117Gly mutant.[43] These results prove that the strong N-dependence of type 1 Cu proteins is due to contributions from backbone amide vibrations rather than from the imidazole ligands.[40] The most likely candidates for the ^{15}N dependence are the amide of the cysteinate ligand, whose N is coplanar with the C_α, C_β, and S_γ atoms of the cysteine moiety[21] and the amides of neighboring residues in the β-sheet.[44]

In contrast to the type 1 Cu proteins, the RR spectrum of Cu_A is largely unaffected by total labeling of the protein by growth on $^{15}NH_4Cl$ (Figures 3C and 5A). Only two vibrational modes show detectable ^{15}N-shifts: -1.6 cm^{-1} at 216 cm^{-1} and -0.4 cm^{-1} at 260 cm^{-1}. The smaller isotope shifts and lower vibrational energies of the N-sensitive modes in Cu_A are more consistent with contributions from Cu−N(Im) vibrations. In addition, the RR spectrum *P. denitrificans* Cu_A (Figure 2) lacks the intense S−C stretching mode of the cysteinate ligand, which is generally observed near 750 cm^{-1} for type 1 Cu proteins.[22] These observations provide strong evidence that the intense ν-(Cu−S) modes at ∼260 and ∼340 cm^{-1} in Cu_A-containing proteins undergo less vibronic and kinematic coupling with the atoms of the cysteinate ligand and the polypeptide backbone than is the case for type 1 Cu proteins. Because the RR spectrum of the Cu_A site is primarily due to vibrations of the Cu_2S_2 cluster and the two terminal His ligands, its frequencies and coordination geometry are more readily simulated by normal coordinate analysis calculations.

Normal Coordinate Analysis. The Cu_A site was approximated by idealized dinuclear models (Figure 6) of the general formula $Cu_2S_2(Im)_2$, with each imidazole ring being treated as a point mass of 67 and each thiolate side chain being approximated by a single sulfur atom. The use of a single S is supported by the apparent lack of kinematic coupling with vibrations of the cysteine side chain, as indicated by the large sulfur-isotope downshifts of 4−5 cm^{-1} and the lack of nitrogen-isotope shifts from the cysteine amide (Figure 5A). The bridging models have the two Cu ions bridged symmetrically by the two cysteine thiolate ligands yielding a planar Cu_2S_2 rhombus as in the crystal structures of Cu_A-containing proteins[15−17] with the imidazole ligands in either a coplanar (B_1)

(39) Blair, D. F.; Campbell, G. W.; Schoonover, J. R.; Chan, S. I.; Gray, H. B.; Malmström, B. G.; Pecht, I.; Swanson, B. I.; Woodruff, W. H.; Cho, W. K.; English, A. M.; Fry, A. F.; Lum, V.; Norton, K. A. *J. Am. Chem. Soc.* **1985**, *107*, 5755−5766.

(40) Sanders-Loehr, J. In *Bioinorganic Chemistry of Copper*; Karlin, K. D., Tyeklár, Z., Eds.; Chapman & Hall: New York, 1993, pp 51−63.

(41) van Pouderoyen, G.; Andrew, C. R.; Loehr, T. M.; Sanders-Loehr, J.; Mazumdar, S.; Hill, H. A. O.; Canters, G. W. *Biochemistry* **1996**, *35*, 1397−1407.

(42) den Blaauwen, T.; Hoitink, C. W. G.; Canters, G. W.; Han, J.; Loehr, T. M.; Sanders-Loehr, J. *Biochemistry* **1993**, *32*, 12455−12464.

(43) Andrew, C. R.; Han, J.; den Blaauwen, T.; van Pouderoyen, G.; Veigenbaum, E.; Canters, G. W.; Sanders-Loehr, J. Manuscript in preparation.

(44) Fraczkiewicz, R.; Fraczkiewicz, G.; Germanas, J.; Czernuszewicz, R. S., unpublished results.

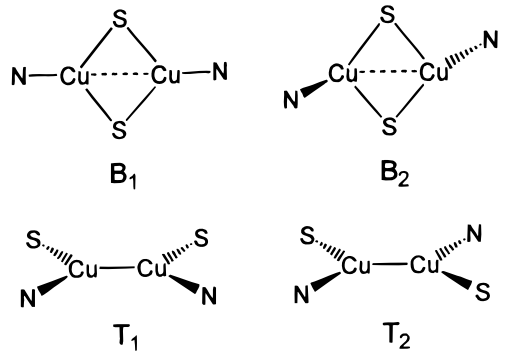

Figure 6. Dinuclear copper coordination geometries investigated as models for Cu_A by normal coordinate analysis. In the B models, the cysteine thiolates are bridging and the histidine imidazoles, denoted by N, are (B_1) colinear with the Cu−Cu axis or (B_2) *trans*-tilted by 40° with respect to the Cu_2S_2 plane. In the T models, the cysteine thiolates are terminal and (T_1) *cis* or (T_2) *trans*.

Table 2. Data Used for Normal Coordinate Analysis of *P. denitrificans* Cu_A with $Cu_2S_2(Im)_2$ Cluster Containing Bridging or Terminal Thiolates[a]

internal coordinate[b]	structural parameters		force constants[c]	
	B_2 model	T_2 model	B_2 model	T_2 model
	bond length (Å)[d]		K (stretching)	
Cu−Cu	2.47	2.47	0.6350	0.3837
Cu−S	2.18	2.18	1.2344	0.9030
Cu−N	1.93	1.93	1.4508	1.4771
	bond angle (deg)[e]		H (bending)	
N−Cu−S	125	120	0.2900[f]	0.2000[f]
S−Cu−Cu	55[g]	120		0.2000[f]
N−Cu−Cu	140[g]	120		0.2000[f]
	torsion angle (deg)[e]		τ (torsion)	
SS(Cu)N[h]	40		0.2200[f]	
SN(Cu)Cu[h]		0		0.100[f]
S−Cu−Cu−S	180	180	0.0200[f]	0.0200[f]
N−Cu−Cu−N	180	180		0.0200[f]
			F (interaction)	
Cu−N:Cu−S			−0.0556	−0.0846
Cu−S:Cu−S			0.1148	0.1068
Cu−N:Cu−N				0.1672
Cu−Cu:Cu−S			−0.2167	
Cu−N:N−Cu−S			0.1473	
Cu−S:N−Cu−S			0.2068	0.0921

[a] Structural parameters and force constants for NCA of the B_2 bridging model (Table 3 and Figure 6) and T_2 terminal model (Table 4 and Figure 6). [b] S of cysteine thiolate. N refers to imidazole with a point mass of 67. [c] Force constants: *K* in mdyn/Å^2, *H* and τ in mdyn/rad^2, and *F* in mdyn/(rad × Å) for stretch-bend. Numerical values were refined against observed frequencies, starting with initial values in ref 36. [d] From EXAFS values for *B. subtilis* Cu_A fragment.[12] [e] Bond angles other than for Cu_2S_2 rhombus set to conform to structures in Figure 6. [f] Fixed force constants, not refined in calculation. [g] Not used as internal coordinates in NCA. [h] Improper torsion, Cu-centered wagging coordinate. Central atom in parentheses.

or tetrahedral (B_2) conformation. The terminal models have a Cu−Cu bonded structure as originally proposed from EXAFS[12] with the terminal cysteine thiolates in either a *cis* (T_1) or *trans* (T_2) conformation. Although the terminal structure has been ruled out by X-ray crystallography, it was included in our analysis to determine whether vibrational spectroscopy can definitively distinguish between bridging and terminal thiolates.

(a) Structural Parameters. The bond distances and bond angles used for NCA of both bridging and terminal models for the vibrational spectrum of *P. denitrificans* Cu_A are shown in Table 2. The metal−ligand bond distances are based on the EXAFS analysis,[12] which appears to give more accurate distances than the current crystal structures at 2.3−2.8-Å resolution.[15−17] The EXAFS metal−ligand distances have an estimated error of ±0.03 Å, whereas even at a resolution of 1.8 Å, the accuracy of M−L bonds in protein crystal structures is believed to be no better than ±0.07 Å.[45] All three crystal structures have been interpreted as showing a distorted tetrahedral geometry about each of the Cu ions, but with significant differences in the degree of distortion (i.e., bond angles) between the two Cu ions. Nevertheless, the complete delocalization of the unpaired electron in the Cu_A site (from the seven-line EPR spectrum) indicates that the two Cu atoms are chemically equivalent.[11] Furthermore, purple CyoA has the same RR signature (intense peaks at 261 and 341 cm^{-1})[29] as *P. denitrificans* Cu_A, suggesting that the structures of their dinuclear copper sites are very similar. Thus, we have made the assumption for our NCA calculations that the two Cu ions in the dinuclear site have the same coordination geometry.

For the bridging models, the bond angles in the Cu_2S_2 rhombus are uniquely defined by the interatomic distances. The imidazole rings were initially assumed to be colinear with the Cu ions as in the B_1 model (Figure 6). However, fits of the vibrational frequencies were significantly improved by tilting the Cu−N(His) vectors while preserving the C_{2h} symmetry (see below). The final stage of force-constant refinement was performed assuming tetrahedrally distorted Cu ions with imidazole groups *trans*-tilted by 40° from the Cu_2S_2 plane as in the B_2 model; the values for this model are listed in Table 2. The terminal cysteinate models, T_1 and T_2 (Figure 6), were both assumed to be planar, and the valence angles Cu−S−N, Cu−Cu−N, and Cu−Cu−S were arbitrarily set equal to 120°. The NCA for these two models is similar, and only the values for the *trans* conformer, T_2, are listed in Table 2.

(b) Force Field Refinement. The **GF**-matrix method[33] and general valence force field were used in the normal mode calculations. The force constants for models B_2 and T_2 (Table 2) were refined against a total of 13 observed Raman frequencies: seven observed fundamentals between 115 and 365 cm^{-1} from natural abundance *P. denitrificans* Cu_A and six frequencies from isotopic shifts in the 138-, 260-, and 339-cm^{-1} modes (Table 1). The 260- and 339-cm^{-1} bands were assigned as totally symmetric modes in the A_g block on the basis of the spectral intensity of their fundamentals and their respective generation of combination and overtone bands (Figure 2). The 138-cm^{-1} band was similarly assigned to the A_g block on the basis of its strong intensity (one-third that at 339-cm^{-1}) with 850-nm excitation.[28] The 216-cm^{-1} band was assigned as a B_u mode in all models, but the isotope shifts of this band were deemed less reliable and thus were excluded from the force field refinement. In each case, the most relevant interaction constants were selected on the basis of their fitting potential (i.e., minimum least squares deviation between observed and calculated frequencies), using our new methodology.[35]

(c) Bridging Model. The best overall fit to the observed RR frequencies and isotope shifts of the *P. denitrificans* Cu_A fragment was obtained using the B_2 model with imidazoles *trans*-distorted by 40° from the Cu_2S_2 plane (Figure 6). Table 3 lists the calculated frequencies, isotope shifts, and potential energy distributions (PED) for each mode. Most importantly, the bridging B_2 model successfully accounts for the intense RR bands at 339 and 260 cm^{-1} as symmetric stretches, recreating both their vibrational energies and requisite large S-isotope dependencies of −5.1 and −4.1 cm^{-1}, respectively. The eigenvectors that correspond to the PEDs in Table 3 are shown in Figure 7. According to these assignments, the first A_g mode at 339 cm^{-1} encompasses a totally symmetric stretch of the Cu_2S_2 rhombus, while the second A_g mode at 260 cm^{-1} has

(45) Guss, J. M.; Bartunik, H. D.; Freeman, H. C. *Acta Crystallogr. B* **1992**, *48*, 790−811.

Table 3. Calculated Frequencies and Isotope Shifts for the B_2 Bridging Model of *P. denitrificans* Cu_A[a]

frequency		Δ^{65}Cu		Δ^{34}S		Δ^{15}N		
obs	calc	obs	calc	obs	calc	obs	calc	PED[b]
						A_g Modes		
339	339.2	1.0	1.9	5.1	5.0	0.0	0.5	Cu−S(77) + Cu−N(27) + Cu−Cu(9)
260	260.2	0.6	1.2	4.1	3.6	0.4	1.0	Cu−N(61) + Cu−S(27) + Cu−Cu:Cu−S(16) + Cu−Cu(10)
138	138.2	1.4	1.7	0.0	0.1	0.0	0.3	Cu−Cu(80) + SS(Cu)N(33) + Cu−S(19) + Cu−N(13)
						B_g Modes		
275	275.0		1.7		4.7		0.0	Cu−S(113)
115	115.0		0.7		1.3		0.4	N−Cu−S(115) + Cu−S(15)
						A_u Modes		
365	365.0		1.8		7.2		0.0	Cu−S(100) + Cu−S:Cu−S(9)
						B_u Modes		
	310.0		2.8		1.9		0.9	Cu−N(56) + Cu−S(39)
216	216.0	0.8	0.2	1.5	3.6	1.6	1.2	Cu−S(50) + Cu−N(47)
	153.4		1.1		1.9		0.2	SS(Cu)N(76) + N−Cu−S(25)

[a] Observed frequencies (in cm^{-1}) and isotoped shifts to lower energy for *P. denitrificans* Cu_A fragment from Table 1. Calculated frequencies and isotope shifts to lower energy from NCA. Input geometry for B_2 bridging model with 40° tetrahedral distortion from Table 2. Force constants (Table 2) were refined against all of the observed frequencies and the A_g mode isotope shifts using a newly developed procedure.[34,35] The three bending modes with calculated frequencies <100 cm^{-1} (see Figure 7) are not listed because that region is difficult to observe experimentally. Because of their uncertainty, the isotope shifts for the B_u mode were not included in the refinement, and those for the A_u and B_g modes are not reported. [b] Calculated potential energy distribution for natural abundance molecule. Only PED contributions from principal force constants >10% are shown.

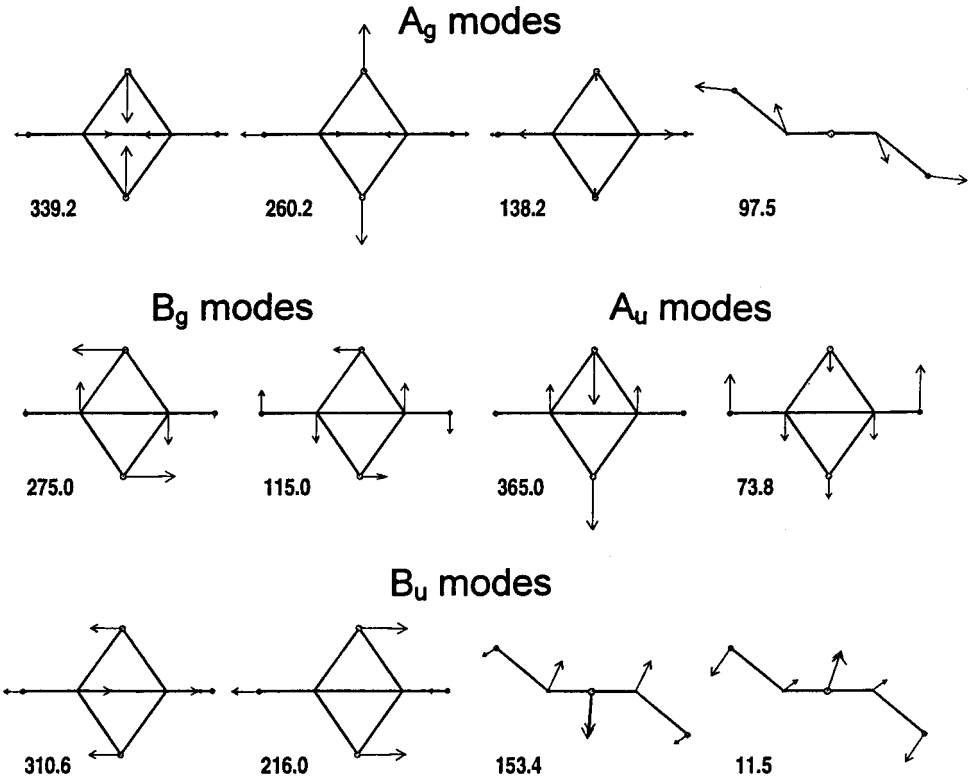

Figure 7. Atomic displacements (eigenvectors) and calculated frequencies (in cm^{-1}) for *P. denitrificans* Cu_A. Assignments are for the B_2 model of a $Cu_2S_2(Im)_2$ cluster with bridging thiolates and terminal imidazoles *trans*-tilted by 40° relative to the planar Cu_2S_2 unit based on the data in Tables 2 and 3. The arrows correspond to unit displacements of normal coordinates using a scaling factor of 5. Due to their projection onto the Cu_2S_2 plane, the N(Im) displacements appear foreshortened.

Cu−N(Im) as well as Cu−S stretching character. The third A_g mode at 138 cm^{-1} is dominated by motions of the two Cu atoms along the Cu···Cu axis.

An additional feature near 216 cm^{-1} is observed in the RR spectra of all of the Cu_A fragments (Figure 2, Table 1). If the force constants are maintained at physically reasonable values for the three previously assigned Ag modes, then the only possible assignments are the first mode of B_g symmetry or the second mode of B_u symmetry (Table 3). However, the B_g mode has higher calculated Cu- and S-isotope dependencies and a total insensitivity to N-isotope substitution. The 216-cm^{-1} vibration observed isotope shifts exhibit a considerably better fit with the B_u mode assignment and can thus be visualized as having opposite distortions for Cu−S and Cu−N (Figure 7).

The B_2 model with a 40° tetrahedral distortion of the imidazoles with respect to the Cu_2S_2 plane was arrived at by examining the effect of varying this angle on the calculated isotope shifts (Figure 8). Of the three A_g modes, the predominantly Cu−Cu stretching motion at 138 cm^{-1} is by far the most sensitive to the Cu−Cu−N angle. A structure with a distortion angle of 0° (i.e., the B_1 model in Figure 6) has a predicted ^{15}N-shift of -1.2 cm^{-1} as compared to the observed shift of 0.0 cm^{-1} (Table 1) and a predicted ^{65}Cu-shift of -0.6 cm^{-1} as compared to the observed shift of -1.4 cm^{-1}. The large N-shift

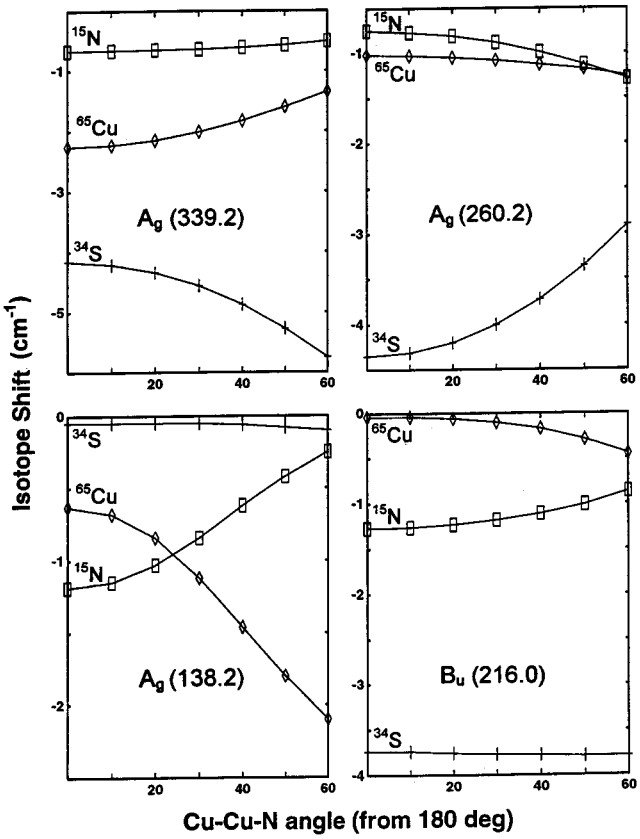

Figure 8. Isotope dependence of A_g and B_u modes as a function of the distortion of the imidazole ligands relative to the planar Cu_2S_2 unit. The distortion angle is calculated as 180° minus the Cu−Cu−N angle, and its variation from 0 to 60° involves a synchronous tetrahedral *trans*-tilting of the two imidazoles. The calculations were performed for the bridging model with the isotopes of Figure 3, varying from the B_1 to the B_2 geometries of Figure 6 while maintaining C_{2h} symmetry.

and small Cu-shift of the 138-cm^{-1} band in the coplanar imidazole structure is due to favorable kinematic coupling between colinear Cu−N and Cu−Cu stretching vibrations. Increasing the distortion angle toward 60° effectively decouples these motions lowering the N-isotope shift and raising the Cu-isotope shift of the 138-cm^{-1} mode closer to their observed values. A smaller, but similar, improvement is observed for the ^{65}Cu- and ^{34}S-shifts of the 339-cm^{-1} mode (Figure 8). However, the calculated ^{34}S-shift of the 260-cm^{-1} mode decreases with increasing distortion angle, taking the shift below the observed value of −4.1 cm^{-1} (Table 1) when the angle reaches 30°. The optimum match of the calculated and observed isotope shifts for the three A_g modes occurs when each of the imidazoles is at an angle of 40° ± 10°, above and below the Cu_2S_2 plane, respectively.

The tetrahedral distortion of the Cu_A site, required by the above NCA calculations, is consistent with the presence of weakly interacting axial ligands, the S of Met227 and backbone carbonyl of Glu218 (Figure 1), which act to repel the imidazole rings from the Cu_2S_2 plane. However, in the crystal structure of *P. denitrificans* Cu_A each imidazole appears to be distorted differently, with distortion angles of 14° and 42° for His224 and His181, respectively.[16] To investigate the effect of inequivalent tetrahedral distortion on the RR spectrum, independent NCA calculations were performed for a lower symmetry (C_s) bridging model where the individual Cu−Cu−N angles were varied independently. For each mode, the angular effect on the isotope shifts was maximized when both angles were changed simultaneously by the same amount. When only one angle was changed, the Cu- and N-isotope shifts of the 138-cm^{-1} mode, for example, never reached the observed values but rather stopped half-way inbetween the values for the B_1 and B_2 models (data not shown). These results make it likely that *both* imidazoles are distinctly distorted by ∼40° from the Cu_2S_2 plane.

Several researchers have raised the possibility of a metal−metal bond in the Cu_A site.[12,28] Although we defined a Cu−Cu internal coordinate in the B_2 model (Table 2), its use was merely a matter of convenience: three independent variables completely define a triangle, hence the Cu−Cu coordinate automatically eliminates redundant bendings of the Cu−Cu−S and Cu−S−Cu valence angles. The Cu−Cu stretch of the 138-cm^{-1} A_g mode is, therefore, fully equivalent to a Cu−S−Cu bend. Either description would be consistent with its large Cu-isotope downshift of ∼2 cm^{-1} (Table 1). Hence, our NCA, by itself, cannot support or rule out the existence of a possible Cu−Cu bond.

(d) Terminal Model. A number of calculations were performed for the T_2 model with *trans* terminal cysteinates (Figure 6). For our initial NCA, we assumed a strong Cu−Cu bond with a force constant of 1.35 mdyn/Å^2 and used an unrefined force field. This led to the prediction of two predominantly Cu−S stretching modes, an A_g at 352 cm^{-1} (^{34}S-shift of −5.3 cm^{-1}) and a B_u at 341 cm^{-1} (^{34}S-shift of −5.8 cm^{-1}). The observed RR spectrum of *P. denitrificans* Cu_A has Cu−S vibrations at 339 cm^{-1} (^{34}S-shift of −5.1 cm^{-1}) and 260 cm^{-1} (^{34}S-shift of −4.1 cm^{-1}). Thus, although the match to the S-isotope shifts is reasonable, this NCA predicts a separation of only 11 cm^{-1} between the two highly S-isotope-dependent modes instead of the observed separation of 81 cm^{-1}. All attempts to reproduce the observed frequency separation by changing assignments or varying the force constants of the other modes were unsuccessful. For cysteines in the *cis* conformation (T_1 model), the results were even worse. Apparently, two Cu−S oscillators separated by a strong Cu−Cu bond are relatively independent and cannot interact sufficiently strongly to produce an ∼80-cm^{-1} separation in frequencies.

We next used a refined force field that predicted a considerably smaller force constant of 0.38 mdyn/Å^2 for the Cu−Cu stretch (Table 2) and led to a completely different set of calculated vibrational frequencies for the T_2 model (Table 4). Although this NCA did accommodate the three intense features of *P. denitrificans* Cu_A at 138, 260, and 339 cm^{-1} as A_g modes, it could not reproduce the observed isotope shifts. The calculated S-isotope shifts were generally too small (ΔS of −1.8 at 339 cm^{-1} and −2.9 at 260 cm^{-1}). The calculated Cu- and N-isotope shifts were generally too large (ΔCu of −3.1 at 339 cm^{-1} and −1.7 at 260 cm^{-1}, ΔN of −1.0 at 339 cm^{-1}). The T_1 model yielded a similar set of calculated frequencies (data not shown). In both cases, varying the force constants yielded no improvement in the predicted isotope dependence. The failure of the T_1 and T_2 models to reproduce the observed pattern of S- and Cu-isotope shifts allows us to unambiguously rule out the terminal cysteinate geometry for *P. denitrificans* Cu_A.

Cu_A Structure and Electron Delocalization. The mononuclear type 1 copper proteins display a surprising array of structures with varying degrees of tetrahedral distortion and ν(Cu−S) values ranging from 430 to 355 cm^{-1}, a spread of 75 cm^{-1}.[22] This fluctuation appears to arise from a variation in the strength of the axial methionine ligand among different proteins, yielding a variable displacement of Cu out of the His_2-Cys ligand plane and related weakening of the Cu−S(Cys) bond. Nevertheless, all of the type 1 copper proteins appear to constrain the methionine ligand away from the copper in order to achieve a trigonal coordination geometry and a lowered

Table 4. Calculated Frequencies and Isotope Shifts for T_2 Terminal Model of *P. denitrificans* Cu_A[a]

frequency		Δ^{65}Cu		Δ^{34}S		Δ^{15}N		
obs	calc	obs	calc	obs	calc	obs	calc	PED
					A_g Modes			
339	339.0	1.0	3.1	5.1	1.8	0.0	1.0	Cu−N(48) + Cu−S(31)
260	260.0	0.6	1.7	4.1	2.9	0.4	0.7	Cu−S(53) + Cu−N(31) + Cu−Cu(13)
138	138.4	1.4	1.1	0.0	1.2	0.0	0.4	Cu−Cu(52) + N−Cu−S(20) + Cu−Cu−N(10)
					B_g Modes			
	102.0		1.3		0.3		0.1	SN(Cu)Cu(100)
					B_u Modes			
	295.6		2.5		1.8		1.0	Cu−N(61) + Cu−S(42)
216	216.2	0.8	0.9	1.5	3.0	1.6	0.8	Cu−S(76) + Cu−N(50)

[a] Values obtained as in Table 3, except that input geometry (Table 2) was for T2 terminal model with cysteinate ligands in a *trans* configuration.

energy barrier for electron transfer.[46] The Cu_A site achieves the same result in a somewhat different fashion. The Cu_2S_2 cluster more strongly limits variations in Cu−S(Cys) bond length and Cu−S−Cu bond angles with the result that the properties of the cluster are less affected by the exact placement of the terminal ligands. Thus, the intense Cu−S stretching vibrations near 260 and 340 cm^{-1} which are the hallmark of purple Cu_A RR spectra, have a spread of only 10 cm^{-1} in the different Cu_A-containing proteins, including the artificial constructs and N_2O reductase.[24,25] Based on calculations for di-μ-oxo-bridged systems,[47] the 10-cm^{-1} spread in the 340-cm^{-1} mode in Cu_A corresponds to a change of <5° in the Cu−S−Cu angle. Consequently, the unusually small Cu−S−Cu angle of ~70° and the resulting short Cu−Cu distance of ~2.5 Å appear to be highly conserved features in Cu_A sites. The greater structural stability of the dinuclear clusters relative to mononuclear sites may provide the evolutionary driving force for the development of Cu_A.

The three-coordinate copper character and effective symmetry of the $Cu_2S_2Im_2$ cluster allow for complete electron delocalization in Cu_A sites, thereby ensuring the small reorganization energy necessary for rapid electron transfer.[48] In Cu_A-containing proteins, the Cu(1.5)−Cu(1.5) state persists even at 10 K. Similar delocalization behavior has been observed for dinuclear Cu in macrocyclic complexes where the only link between the coppers appears to be a Cu−Cu bond[49,50] and for the dithiolate-bridged $[Cu_2(iPrdacos)_2]^+$ complex with a Cu···Cu distance of 2.9 Å.[51] The tri-μ-OH-bridged $[Fe_2(OH)_3(tmtacn)_2]^{2+}$ complex is also a fully delocalized Fe(2.5)−Fe(2.5) system where the Fe···Fe distance of 2.51 Å suggests some contribution from metal−metal bonding.[52] A surprising feature of the Cu_A-containing proteins is that the $Cu_2S_2Im_2$ cluster achieves the fully delocalized state despite the slight asymmetry in the two Cu sites arising from the Met227 and Glu218 ligands (Figure 1) and the ENDOR evidence for two different His ligand environments.[53] Furthermore, this fully delocalized structure is readily formed in synthetic constructs where a second Cys ligand has been added to a quinol oxidase, azurin, or amicyanin.[7−9] However, any more substantial changes in the terminal ligands of the Cu_A cluster, such as replacement of Met227 with Ile,[54] causes the system to revert to a trapped-valence, Cu(I)−Cu(II) state.

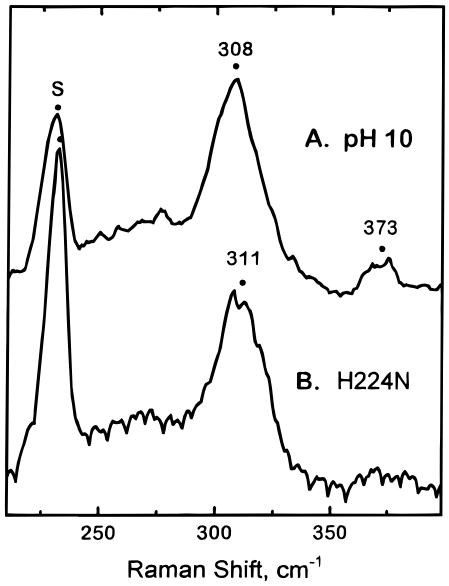

Figure 9. RR spectra of type 2 sites generated in *P. denitrificans* Cu_A fragment. (A) Wild-type Cu_A (2.6 mM protein) in 40 mM CHES (pH 10). (B) His224Asn mutant of Cu_A (2.9 mM protein) in 20 mM Bis-Tris (pH 6.5). Spectra measured at 15 K using 350.8-nm excitation (10 mW), 7-cm^{-1} resolution and 8 scans.

Raising the pH to 10 causes a similar loss of electron delocalization in the *P. denitrificans* Cu_A fragment, resulting in the formation of a distinct Cu(II) species.[3] Both copper atoms remain coordinated, and the reaction is fully reversible by returning to pH 7. The Cu(II) component has the optical, EPR, and RR characteristics of a type 2 Cu site. It exhibits an absorption maximum at 370 nm[3] and a single low-energy Cu−S stretch at 311 cm^{-1} (Figure 9B). The low frequency of this vibrational mode indicates the presence of long (~2.25 Å) Cu−S bonds due either to a tetragonal coordination geometry with four strong ligands[22] or to the sulfur being more weakly coordinated to each Cu because its bonding is shared with a second Cu. The alkaline pH effect on the *P. denitrificans* Cu_A fragment is reminiscent of the His117Gly ligand mutant of azurin that forms a type 2 Cu site at pH 9.0 with a single ν-(Cu−S) mode at 312 cm^{-1}.[42] In the azurin mutant, it is likely that two hydroxide ions have added to the Cu(II) to generate a

(46) Guckert, J. A.; Lowery, M. D.; Solomon, E. I. *J. Am. Chem. Soc.* **1995**, *117*, 2817−2844.
(47) Wing, R. M.; Callahan, K. P. *Inorg. Chem.* **1969**, *8*, 871−874.
(48) Ramirez, B. E.; Malmström, B. G.; Winkler, J. R.; Gray, H. B. *Proc. Natl. Acad. Sci. U.S.A.* **1995**, *92*, 11949−11951.
(49) Barr, M. E.; Smith, P. H.; Antholine, W. E.; Spencer, B. *J. Chem. Soc. Chem. Commun.* **1993**, 1649−1652.
(50) Harding, C.; Nelson, J.; Symons, M. C. R.; Wyatt, J. *J. Chem. Soc. Chem. Commun.* **1994**, 2499−2500.
(51) Houser, R. P.; Young, V. G., Jr.; Tolman, W. B. *J. Am. Chem. Soc.* **1996**, *118*, 1201−1206.
(52) Gamelin, D. R.; Bominaar, E. L., Kirk, M. L.; Wieghardt, K.; Solomon, E. I. *J. Am. Chem. Soc.* **1996**, *118*, 8085−8097.
(53) Gurbiel, R. J.; Fann, Y.-C.; Surerus, K. K.; Werst, M. M.; Musser, S. M.; Doan, P. E.; Chan, S. I.; Fee, J. A.; Hoffman, B. M. *J. Am. Chem. Soc.* **1993**, *115*, 10888−10894.
(54) Zickermann, V.; Verkhovsky, M.; Morgan, J.; Wikström, M.; Anemüller, S.; Bill, E.; Steffens, G. C. M.; Ludwig, B. *Eur. J. Biochem.* **1995**, *234*, 506−512.

tetragonal site with four strong ligands: Cys, His, and two OH^-. For the high pH form of Cu_A, it is likely that a single hydroxide has added to one of the copper atoms to generate a tetrahedral Cu(II) site with two bridging Cys, a terminal His, and a terminal OH^-.

Destruction of the Cu_A-site symmetry by removal of one of the histidine ligands also prevents electron delocalization. Thus, conversion of His224 to Asn (previously referred to as residue 252) in the *P. denitrificans* Cu_A fragment yields a trapped-valence Cu(I)−Cu(II) site containing a type 2 Cu(II)-cysteinate with a λ_{max} at 370 nm[14] and a Cu−S stretch at 308 cm^{-1} (Figure 9A). Its similarity to the high-pH form of Cu_A suggests that the His224Asn mutant also has a tetrahedral Cu(II) coordinated with the two original bridging Cys and one or two aqua ligands to compensate for the lost His. This shows that each of the copper atoms in a Cu_A site needs to have a strong terminal His ligand in order to achieve the copper equality required for valence delocalization.

Conclusions

Resonance Raman spectroscopy and normal coordinate analysis have proven to be a powerful tools for obtaining detailed structural information about the Cu_A site of cytochrome *c* oxidase. The combination of EXAFS-determined interatomic distances and geometric constraints imposed by the isotopic shifts of RR bands has led to a more detailed structure of the Cu_A site than can be achieved by X-ray crystallography alone.

(1) The RR spectroscopic properties of Cu_A (especially the S-, Cu-, and N-isotope shifts) are best explained by a site containing two copper ions bridged by two cysteine thiolates and coordinated to two terminal histidine imidazoles, as in the X-ray crystal structure. The alternative structure with only a Cu−Cu bond and terminal thiolate and imidazole ligands can be definitely ruled out by this vibrational analysis.

(2) The most intense bands at 339, 260, and 138 cm^{-1} in the RR spectrum of the *P. denitrificans* Cu_A fragment are assigned to symmetric stretches involving primarily the Cu−S, Cu−N(Im), and Cu−Cu moieties, respectively. Due to coordinate redundancy, the large Cu-isotope shift of the 138-cm^{-1} band can be equally well attributed to either a Cu−Cu stretching vibration or a Cu−S−Cu bending vibration. Thus, RR data and NCA alone cannot definitively confirm or rule out the existence of a Cu−Cu bond in the Cu_A site.

(3) Isotope shifts are of key importance in assigning the vibrational spectrum of Cu_A. Our NCA shows that the degree of vibrational kinematic coupling is particularly sensitive to the orientation of the imidazole ligands and that different coordination geometries lead to different isotope behavior. The observed isotope dependence of the Cu_A site is most consistent with a tetrahedral geometry in which the two imidazole ligands are *trans*-tilted by ∼40° above and below the Cu_2S_2 plane, respectively.

(4) The similar RR spectroscopic signature for all Cu_A sites indicates a highly conserved structure for the Cu_2S_2 core in both native proteins and constructs, requiring a short Cu−Cu distance of ∼2.5 Å and narrow Cu−S−Cu angle of ∼70°. This thermodynamically favored core structure also facilitates complete sharing of the unpaired electron between the two copper atoms such that the species remains valence-delocalized even at 10 K. Perturbation of the terminal ligands by raising the pH or mutation of the His224 ligand to Asn causes enough inequivalence of the two copper atoms for the site to revert to a trapped-valence, Cu(I)−Cu(II) state.

Acknowledgment. We are grateful to Drs. Thomas M. Loehr, William H. Woodruff, and Stacie Wallace-Williams for helpful discussions. This research was supported by the National Institutes of Health, Grants GM 18865 (J.S.-L.) and GM 48370 (R.S.C.), the EC, Grant SC1-CT91-0698 (M.S.), and the Academy of Finland (P.L.).

Supporting Information Available: Numerical solution for the eigenvectors in Figure 7 in the animation XYZ format readable by program X-MOL.[37] See any current masthead page for Internet access instructions.

JA960969G